

# Leakage Suppression for Holonomic Quantum Gates

Bao-Jie Liu<sup>1,2</sup> and Man-Hong Yung<sup>2,\*</sup>

<sup>1</sup>*Department of Physics, Harbin Institute of Technology, Harbin 150001, China*

<sup>2</sup>*Institute for Quantum Science and Engineering, and Department of Physics, Southern University of Science and Technology, Shenzhen 518055, China*

(Dated: August 7, 2022)

Non-Abelian geometric phases acquired in cyclic quantum evolutions can be utilized as natural resources for constructing robust holonomic gates for quantum information processing. Recently, an extensible holonomic quantum computation (HQC) was proposed and demonstrated in a recent superconducting experiment [T. Yan et al., Phys. Rev. Lett. 122, 080501 (2019)]. However, for the weakly anharmonic system, this HQC was given of low gate fidelity due to leakage to states outside of the computational subspace. Here, we propose a scheme that nonadiabatic holonomic gates can be constructed via dynamical invariant using resonant superconducting interaction of three-level quantum systems. Furthermore, we can be compatible with optimal control technology for maximizing the gate fidelity against leakage error. For benchmarking, we provide a thorough analysis on the performance of our scheme under experimental conditions; we found that both the gate error can be reduced by as much as 91.7% compared with conventional HQC. Furthermore, the leakage rates can be reduced to  $10^{-4}$  level by numerically choosing suitable control parameter. Therefore, our scheme provides a promising way towards fault-tolerant quantum computation in a weakly anharmonic solid-state system.

## I. INTRODUCTION

Quantum computation is considered to be a promising solution to some complex problems [1, 2], which will be very beneficial to many practical applications in quantum information processing [3–5]. However, due to inevitable noise and operational errors, constructing precise quantum control is challenging in practice. Consequently, how to construct high-fidelity and noise-resistant quantum gates are of fundamental importance to quantum computation. Geometric quantum computation (GQC) [6–14] takes a different approach, which utilizes an unique property of quantum theory: the quantum state will acquire an Abelian or non-Abelian geometric phase after a cyclic evolution in non-degenerate or degenerate space. An important property of geometric phase depends only on the overall properties of the evolutionary trajectory [10–12]. Therefore, quantum gates based on the geometric phases are robust to local control errors during a quantum evolution [13, 14]. Specifically, the geometric phase can be divided into a commutative real number, known as the adiabatic Berry phase [15] or nonadiabatic A-A phase [16], or a non-commutative matrix (non-Abelian holonomy) [17, 18] that is the key ingredient in constructing quantum operations for holonomic quantum computation (HQC) [6].

Previous applications of holonomic quantum computing (HQC) [19–21] need to meet adiabatic condition to avoid transitions between different sets of eigenstates. However, adiabatic conditions imply lengthy quantum gate operation time. Therefore, adiabatic HQC is severely limited by decoherence caused by the environment noises [22–24]. It was later discovered that if we construct a driving Hamiltonian with time-independent eigenstates and establish a holonomic gate, we can achieve nonadiabatic holonomic quantum computation (NHQC) [25–36]. However, this condition imposes strin-

gent requirements on the driving Hamiltonian; the systematic errors would introduce additional fluctuating phase shifts, smearing the geometric phases [38–40]. Recently, a flexible nonadiabatic holonomic quantum computation (NHQC+) [41] was proposed to avoid the constraints of NHQC and improve the robustness against systematic errors. However, existing NHQC+ [41–44] cannot solve the leakage error caused by the presence of noncomputational levels when driven by control pulses in many physical quantum systems such as superconducting qubits [42].

Here, we shall demonstrate a scheme that nonadiabatic holonomic gates can be realized via dynamical invariant [45] in a resonant three-level quantum systems of superconducting qubit. In this way, our scheme maintains both flexibility and robustness against certain types of noises. Furthermore, it can further be compatible with optimal control technology to the leakage error for realizing maximizing the gate fidelity. For benchmarking, we provide a thorough analysis on the performance of our scheme with recent experimental parameters; we found that the leakage rates can be reduced below  $10^{-4}$  by choosing proper optimal parameter, which is greatly improved compared with conventional nonadiabatic holonomic quantum gates [35, 42].

## II. THE BASIC MODEL

Here we consider a superconducting Xmon system demonstrated in Ref. [35, 42], which has a weakly anharmonic potential. The lowest four energy levels of our Xmon qutrit are described by  $|g\rangle$ ,  $|e\rangle$ ,  $|f\rangle$  and  $|h\rangle$ , as shown in Fig. 1(a). Here, the ground state  $|g\rangle \equiv |0\rangle$  and the second excited state  $|f\rangle \equiv |1\rangle$  form our qubit, and the first excited state  $|e\rangle$  and third excited state  $|h\rangle$  denote noncomputational state. The system is resonantly driven by two microwave pulses to realize the transitions of  $|0\rangle \leftrightarrow |e\rangle$  and  $|e\rangle \leftrightarrow |1\rangle$ . The system Hamiltonian in the basis  $\{|g\rangle, |e\rangle, |f\rangle, |h\rangle\}$  is given by (here

\* yung@sustech.edu.cn

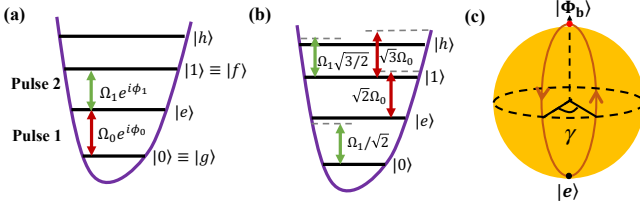


FIG. 1. Illustration of our proposed implementation. (a) HQC scheme using resonate three levels of an superconducting Xmon qubit as proposed in this work. Two pulses with Rabi frequencies of  $\Omega_0(t)$  and  $\Omega_1(t)$  are used. (b) Cross coupling and leakage to higher level in a many-level system with weak anharmonicity  $\alpha$  in an Xmon type of superconducting device. For example, the Stokes pulse  $\Omega_1$  that resonantly couples  $|e\rangle$  and  $|1\rangle$  in (a) can now also introduce an off-resonant coupling between  $|0\rangle$  and  $|e\rangle$  in an Xmon. (c) Conceptual explanation for holonomic quantum gate.

and after  $\hbar \equiv 1$ )

$$H = \begin{pmatrix} 0 & f & 0 & 0 \\ f & \omega_0 & \sqrt{2}f & 0 \\ 0 & \sqrt{2}f & \omega_1 & \sqrt{3}f \\ 0 & 0 & \sqrt{3}f & \omega_2 \end{pmatrix}, \quad (1)$$

where the pulse field  $f = \Omega_0 \cos(\omega_0 t + \phi_0) + \frac{\Omega_1}{\sqrt{2}} \cos(\omega_1 t - \phi_1)$  with the driving amplitude  $\Omega_{0,1}(t)$ , frequency  $\omega_{0,1}$ , and phase  $\phi_{0,1}(t)$ . The corresponding transition energies are expressed by  $\omega_{0,1,2}$ , with the ground energy set to zero, and the intrinsic anharmonicity of the Xmon system is taken as  $\alpha = \omega_1 - \omega_0$ . Here, using the rotating wave approximation and moving to the interaction frame, the Hamiltonian is written as

$$H_I = \frac{1}{2} \begin{pmatrix} 0 & \Omega_0 e^{i\phi_0} & 0 & 0 \\ \Omega_0 e^{-i\phi_0} & 0 & \Omega_1 e^{-i\phi_1} & 0 \\ 0 & \Omega_1 e^{i\phi_1} & 0 & 0 \\ 0 & 0 & 0 & 0 \end{pmatrix} + H_{\text{leak}}, \quad (2)$$

where  $H_{\text{leak}}$  described the cross coupling and leakage caused by higher excited energy, as shown in Fig. 1(b), which is given by

$$H_{\text{leak}} = \frac{\sqrt{2}}{2} \begin{pmatrix} 0 & \frac{\Omega_1}{2} e^{-i(\phi_1 + \alpha t)} & 0 & 0 \\ \frac{\Omega_1}{2} e^{i(\phi_1 + \alpha t)} & 0 & \Omega_0 e^{-i(\phi_0 - \alpha t)} & 0 \\ 0 & \Omega_0 e^{i(\phi_0 - \alpha t)} & 0 & 0 \\ 0 & 0 & M^* & 0 \end{pmatrix}. \quad (3)$$

where  $M \equiv \sqrt{3/2}\Omega_0 e^{-i(\phi_0 - 2\alpha t)} + \frac{\sqrt{3}\Omega_1}{2} e^{-i(\phi - \alpha t)}$ . For the case  $|\alpha| \gg |\Omega_{0,1}|$ , the term  $H_{\text{leak}}$  averages out to zero.

For our purpose, we assume that  $\Omega_0(t)$  and  $\Omega_1(t)$  have the same time dependence, which means the time-dependent driving amplitude can be parameterized as  $\Omega_0(t) = \Omega(t) \sin \frac{\theta}{2}$ ,  $\Omega_1(t) = \Omega(t) \cos \frac{\theta}{2}$ ; the time-independent relative phase is set as  $\phi = \phi_1(t) - \phi_0(t)$ . Consequently, the effective Hamiltonian can be given by

$$H_e(t) = \Omega(t) \cos \phi_0(t) \hat{T}_1 + \Omega(t) \sin \phi_0(t) \hat{T}_2. \quad (4)$$

where  $\hat{T}_1 \equiv (|\Phi_b\rangle\langle e| + H.c.)/2$ ,  $\hat{T}_2 \equiv (i|\Phi_b\rangle\langle e| + H.c.)/2$ , and  $\hat{T}_3 \equiv (|\Phi_b\rangle\langle \Phi_b| - |e\rangle\langle e|)/2$  are the  $SU(2)$  algebra of

unitary  $2 \times 2$  matrices, obeying the following commutation relation  $[\hat{T}_a, \hat{T}_b] = i\epsilon^{abc}\hat{T}_c$ ; the time-independent bright state  $|\Phi_b\rangle \equiv \sin(\theta/2)|0\rangle + \cos(\theta/2)e^{i\phi}|1\rangle$  is orthogonal to the excited state  $|e\rangle$ . Note that dark state  $|\Phi_d\rangle = \cos(\theta/2)|0\rangle - \sin(\theta/2)e^{i\phi}|1\rangle$  is now decoupled from states  $|\Phi_b\rangle$  and  $|e\rangle$ .

For the  $SU(2)$  dynamical symmetry Hamiltonian  $H_e(t)$  in Eq. (4), the dynamical invariant  $I(t)$ , such that  $\frac{dI}{dt} \equiv \frac{\partial I}{\partial t} + \frac{1}{i\hbar} [I, H] = 0$ , is given by

$$I(t) = \frac{G_0}{2} \left( \cos \eta \sin \chi \hat{T}_1 + \sin \eta \sin \chi \hat{T}_2 + \cos \chi \hat{T}_3 \right) \\ = \frac{G_0}{2} \begin{pmatrix} \cos \chi & \sin \chi e^{-i\eta} \\ \sin \chi e^{i\eta} & -\cos \chi \end{pmatrix} \quad (5)$$

where  $G_0$  is an arbitrary constant to make  $I(t)$  dimensionless, and the time-dependent auxiliary parameters  $\chi$  and  $\eta$  satisfy the differential equations,

$$\Omega(t) = \frac{\dot{\chi}}{\sin(\phi_0 - \eta)}, \quad \phi_0(t) = \eta - \arctan\left(\frac{\dot{\chi}}{\eta \tan \chi}\right). \quad (6)$$

The eigenvectors of the invariant are given by  $|\mu_0(t)\rangle = (\cos \frac{\chi}{2} e^{-i\frac{\eta}{2}}, \sin \frac{\chi}{2} e^{i\frac{\eta}{2}})^T$  and  $|\mu_1(t)\rangle = (\sin \frac{\chi}{2} e^{-i\frac{\eta}{2}}, -\cos \frac{\chi}{2} e^{i\frac{\eta}{2}})^T$ .

### III. HOLONOMIC QUANTUM GATE VIA DYNAMICAL INVARIANT

To construct holonomic gates, we choose an eigenvector  $|\mu_1(t)\rangle$  of dynamical invariant as auxiliary states, which satisfy the following conditions [41] of (i) the cyclic evolution  $\Pi_1(0) = \Pi_1(\tau) = |\Phi_b\rangle\langle \Phi_b|$  with  $\chi(0) = \chi(\tau) = \pi$ , and (ii) the von Neumann equation  $\frac{d}{dt} \Pi_k(t) = -i[H_1(t), \Pi_k(t)]$ , where  $\Pi_k(t) \equiv |\mu_k(t)\rangle\langle \mu_k(t)|$  denotes the projector of the auxiliary basis, (iii) the elimination of dynamical phase  $\gamma_d = \int_0^\tau \langle \mu_1(t) | H_e(t) | \mu_1(t) \rangle dt = 0$ .

Now, we demonstrate how to build up universal arbitrary holonomic single-qubit gates. Here, we choose the auxiliary parameters  $\chi(t) = \frac{\pi}{2} [1 - \cos(\frac{2\pi t}{\tau})]$  for a cyclic evolution. After the evolution, the state  $|\mu_1\rangle$  gains a global phase  $\gamma$ , i.e.,  $|\mu_1(\tau)\rangle = e^{-i\gamma} |\mu_1(0)\rangle$  including both geometric phase  $\gamma_g$  and dynamical phase  $\gamma_d$ . The pure geometric phases  $\gamma = \eta_g$  can be obtained by using the spin-echo technique by setting  $\eta(t) = -\frac{2\pi}{5} \sin(\frac{\pi t}{\tau}) \cos(\frac{\pi t}{\tau}) - \frac{\pi}{2}$  and  $\eta(t) = \frac{2\pi}{5} \sin(\frac{\pi t}{\tau}) \cos(\frac{\pi t}{\tau}) - \frac{\pi}{2} - \eta_g$  for two intervals,  $(0, \tau/2)$  and  $(\tau/2, \tau)$  to erase the accumulated dynamical phase, as shown in Fig. 1(c). As a result, the final time evolution operator on the subspace  $\{|\Phi_b\rangle, |\Phi_d\rangle\}$  is given by  $U(\tau) = e^{i\gamma} |\Phi_b\rangle\langle \Phi_b| + |\Phi_d\rangle\langle \Phi_d|$ . Consequently, the holonomic gate can be spanned by the logical  $\{|0\rangle, |1\rangle\}$  basis as,

$$U(\theta, \phi, \gamma) = \begin{pmatrix} c_{\frac{\gamma}{2}} - i s_{\frac{\gamma}{2}} c_\theta & -i s_{\frac{\gamma}{2}} s_\theta e^{i\phi_1} \\ -i s_{\frac{\gamma}{2}} s_\theta e^{-i\phi} & c_{\frac{\gamma}{2}} + i s_{\frac{\gamma}{2}} c_\theta \end{pmatrix}, \quad (7) \\ = \exp\left(-i\frac{\gamma}{2} \mathbf{n} \cdot \boldsymbol{\sigma}\right)$$

where  $c_x \equiv \cos x$  and  $s_x \equiv \sin x$ . This operation corresponds to a rotation around the axis  $\mathbf{n} =$

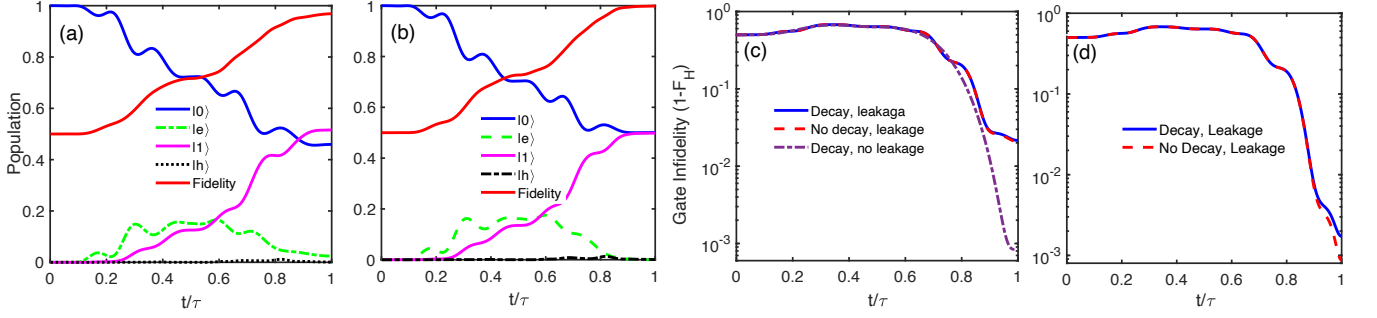


FIG. 2. Illustration of the performance of the proposed single gates. States population and fidelity dynamics of (a) holonomic Hadamard gate and (b) optimal holonomic Hadamard gate, as a function of  $t/\tau$  with the initial state being  $|0\rangle$ . The dynamics of the gate infidelities of (c) holonomic Hadamard gate and (d) optimal holonomic Hadamard gate with different settings of decay and leakage parameters.

$(\sin \theta \cos \phi, \sin \theta \sin \phi, \cos \theta)$  by an angle of  $\gamma$ , which picks up a global phase  $\gamma/2$ . Therefore, it is feasible to implement the unconventional holonomic gate by designing particular  $\phi$  and  $\gamma$ .

When considering the realistic case, i.e., taking the decoherence effect into consideration, the performance of a holonomic gate in Eq. (7), induced from the Hamiltonian in Eq. (2), can be evaluated by using a master equation in the Lindblad form [46] as,

$$\dot{\rho}(t) = i[\rho(t), H_I(t)] + \frac{1}{2} [\Gamma_1 \mathcal{L}(\lambda^+) + \Gamma_2 \mathcal{L}(\lambda^z)], \quad (8)$$

where  $\rho(t)$  is the density matrix of the considered system and  $\mathcal{L}(A) = 2A\rho_1 A^\dagger - A^\dagger A\rho_1 - \rho_1 A^\dagger A$  is the Lindbladian of the operator  $A$ ,  $\lambda^+ = |0\rangle\langle e| + \sqrt{2}|e\rangle\langle 1| + \sqrt{2}|1\rangle\langle h|$ , and  $\lambda^z = |e\rangle\langle e| + 2|1\rangle\langle 1| + 3|h\rangle\langle h|$ . In addition  $\Gamma_1^j$  and  $\Gamma_2^j$  are the decay and dephasing rates of the  $\{0, 1, e, h\}$  four-level systems, respectively. In our simulation, we have used the following set of experimental parameters. The anharmonicity and gate time is set as  $\alpha = 2\pi \times 225$  MHz,  $\tau = 30$  ns, and  $\Gamma_1^j = \Gamma_2^j \approx 2\pi \times 4$  kHz [47, 48]. Suppose that the qubit is initially prepared in the  $|\psi(0)\rangle = |0\rangle$  state, the time-dependence of the state populations and the state fidelity of realizing the holonomic Hadamard gate are depicted in Fig. 2a, where the state fidelity  $F = |\langle\psi_I|\psi(\tau)\rangle|^2$  are obtained to be 96.86% with the ideal state  $|\psi_I\rangle = \frac{1}{\sqrt{2}}(|0\rangle + |1\rangle)$ . Furthermore, we have also investigated the gate fidelity  $F_H$  of the Hadamard gate for initial states of the form  $|\psi\rangle = \cos \Theta|0\rangle + \sin \Theta|1\rangle$ , where a total of 1001 different values of  $\Theta$  were uniformly chosen in the range of  $[0, 2\pi]$ , as shown in Fig. 2c. The gate fidelity  $F_H$  of the Hadamard is 97.84% with the experimental parameters.

To analyze the major sources of error that reduce fidelity, we firstly consider the effect of decoherence by setting  $\Gamma_{1,2} = 0$ . From the Fig. 2c, we found that decoherence has very little effect on the low fidelity. Next, to investigate the effect of higher energy levels and unwanted transitions due to the weakly anharmonicity, we set  $H_{\text{leak}} = 0$  but with the decoherence, and get the gate fidelity as high as  $F_H = 99.92\%$ . Therefore, we are able to construct an error budget with leakage error 96.3% and decoherence 3.7% by using the contribution to the total error in percent.

#### IV. ELIMINATION OF LEAKAGE VIA OPTIMAL CONTROL

To overcome the problem, we demonstrate that modifying the pulses via the optimal control technology, one can effectively suppress these unwanted effects and leakage and achieve the desired holonomic gate with high fidelity. Here, we propose a scheme by adding the different quadrature components for two pulses of  $\Omega_{0,1}(t)$  to suppress this leakage and overlap coupling noises. We suppose the optimal control ansatz function is given by

$$\tilde{\Omega}_0(t) = (1 + i\beta_1)\Omega_0(t), \quad \tilde{\Omega}_1(t) = (1 + i\beta_2)\Omega_1(t) \quad (9)$$

where  $\beta_1$  and  $\beta_2$  are the optimal parameters.

Here, we can numerically adjust the parameters  $\beta_{1,2}$  to minimum the leakage error. We choose  $\beta_1 = -0.3$  and  $\beta_2 = -0.055$  for the above setting of  $\alpha = 2\pi \times 225$  MHz and  $\tau = 30$  ns. With the optimal control, we find the state and gate

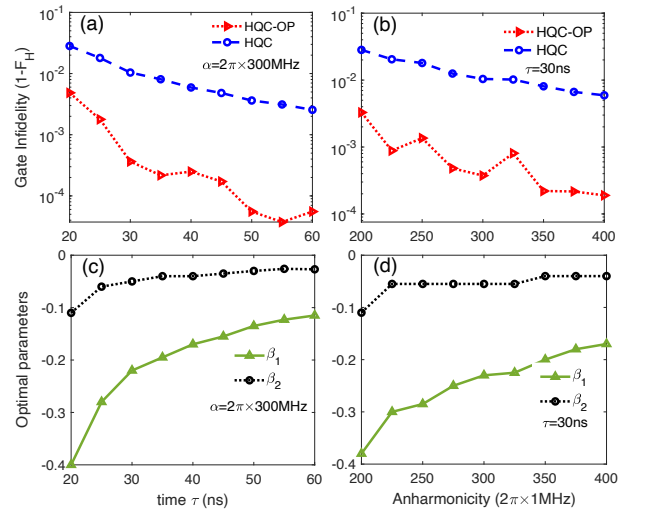


FIG. 3. The holonomic gate infidelities of Hadamard gate with and without optimal control as functions of (a) time  $\tau$  and (b) anharmonicity  $\alpha$ . The optimal parameters  $\beta_{1,2}$  vary with (c) time  $\tau$  and (d) anharmonicity  $\alpha$ .

fidelity of holonomic Hadamard gate can greatly improved from  $F_H = 96.86\%$  and  $F_H = 97.84\%$  to  $F_H = 99.85\%$  and  $F_H = 99.82\%$ , as shown in Fig. 2b and 2d. Furthermore, we find the leakage error rate is below  $10^{-3}$  level without considering relaxation.

To further illustrate the practicality of our optimized control method, we plot the gate fidelities as functions of the gate time  $\tau$  and anharmonicity  $\alpha$  of the Xmon qubit in the Fig. (3)a and (3)b, where we can find that the gate fidelities of the holonomic H gate can always be improved by choosing appropriate parameters  $\beta_1$  and  $\beta_2$  as given by the Table I. When  $\alpha = 2\pi \times 300$  MHz and  $\tau = 55$  ns, the leakage error rate can be below  $10^{-4}$  level. At the same time, we can see that the optimal parameters are getting closer to zero as the Rabi amplitude decreases and the anharmonicity increases as shown in the Fig. (3)c and (3)d.

TABLE I. Optimal pulses with the control parameters  $\beta_{1,2}$  for different gate time  $\tau$  with  $\alpha = 2\pi \times 300$  MHz, and different anharmonicities with  $\tau = 30$  ns.

| $\tau$        | 20   | 25    | 30    | 35    | 40    | 45    | 50    | 55    | 60    |
|---------------|------|-------|-------|-------|-------|-------|-------|-------|-------|
| $-\beta_1$    | 0.4  | 0.28  | 0.22  | 0.195 | 0.170 | 0.155 | 0.135 | 0.123 | 0.115 |
| $-\beta_2$    | 0.11 | 0.06  | 0.05  | 0.04  | 0.04  | 0.035 | 0.03  | 0.026 | 0.027 |
| $\alpha/2\pi$ | 200  | 225   | 250   | 275   | 300   | 325   | 350   | 375   | 400   |
| $-\beta_1$    | 0.38 | 0.3   | 0.285 | 0.25  | 0.230 | 0.225 | 0.2   | 0.180 | 0.17  |
| $-\beta_2$    | 0.11 | 0.055 | 0.055 | 0.055 | 0.055 | 0.04  | 0.04  | 0.04  | 0.034 |

## V. CONCLUSION

In this paper, we have demonstrated a new scheme that dynamical-invariant based nonadiabatic holonomic gate can be constructed with a three-level system on a weakly anharmonic superconducting Xmon qubit. Moreover, we can be compatible with optimal control technology to minimum leak error for greatly improving the gate fidelity. Numerical simulation shows that the leakage rates can be reduced to  $10^{-4}$  level by choosing suitable control parameter. Our HQC scheme provides a promising way towards fault-tolerant quantum computation in a realistic solid-state system.

## ACKNOWLEDGMENTS

This work is supported by the Key-Area Research and Development Program of Guangdong Province (Grant No.2018B030326001), the National Natural Science Foundation of China (Grant No.11875160 and No.11874156), the Natural Science Foundation of Guangdong Province (Grant No.2017B030308003), the National Key R& D Program of China (Grant No.2016YFA0301803, the Guangdong Innovative and Entrepreneurial Research Team Program (Grant No.2016ZT06D348), the Economy, Trade and Information Commission of Shenzhen Municipality (Grant No.201901161512), the Science, Technology and Innovation Commission of Shenzhen Municipality (Grant No. JCYJ20170412152620376, No. JCYJ20170817105046702, and No. KYTDP20181011104202253).

- 
- [1] P. W. Shor, Polynomial-Time Algorithms for Prime Factorization and Discrete Logarithms on a Quantum Computer, SIAM J. Comput. **26**, 1484 (1997).
  - [2] L. K. Grover, Quantum Mechanics Helps in Searching for a Needle in a Haystack, Phys. Rev. Lett. **79**, 325 (1997).
  - [3] M. A. Nielsen and I. L. Chuang, Quantum Computation and Quantum Information (Cambridge University Press, 2000).
  - [4] J. I. Cirac and P. Zoller, Quantum Computations with Cold Trapped Ions, Phys. Rev. Lett. **74**, 4091 (1995).
  - [5] Q. A. Turchette, C. J. Hood, W. Lange, H. Mabuchi, and H. J. Kimble, Measurement of conditional phase shifts for quantum logic, Phys. Rev. Lett. **75**, 4710 (1995).
  - [6] P. Zanardi, and M. Rasetti, Holonomic quantum computation, Phys. Lett. A **264**, 94 (1999).
  - [7] E. Sjöqvist, Trend: A new phase in quantum computation, Physics **1**, 35 (2008).
  - [8] Wang, X. B., and M. Keiji, Nonadiabatic conditional geometric phase shift with NMR, Phys. Rev. Lett. **87**, 097901 (2001).
  - [9] S.-L. Zhu, and Z. D. Wang, Implementation of universal quantum gates based on nonadiabatic geometric phases. Phys. Rev. Lett. **89**, 097902 (2002).
  - [10] S.-L. Zhu, and P. Zanardi, Geometric quantum gates that are robust against stochastic control errors, Phys. Rev. A **72**, 020301(R) (2005).
  - [11] S. Berger, M. Pechal, A. A. Abdumalikov, Jr. C. Eichler, L. Steffen, A. Fedorov, A. Wallraff, and S. Filipp, Exploring the effect of noise on the Berry phase, Phys. Rev. A **87**, 060303(R) (2013).
  - [12] G. D. Chiara and G. M. Palma, Berry phase for a spin-1/2 particle in a classical fluctuating field, Phys. Rev. Lett. **91**, 090404 (2003).
  - [13] P. J. Leek, J. M. Fink, A. Blais, R. Bianchetti, M. Gppl, J. M. Gambetta, D. I. Schuster, L. Frunzio, R. J. Schoelkopf, and A. Wallraff, Observation of Berry's phase in a solid state qubit, Science **318**, 1889 (2007).
  - [14] S. Filipp, J. Klepp, Y. Hasegawa, C. Plonka-Spehr, U. Schmidt, P. Geltenbort, and H. Rauch, Experimental demonstration of the stability of Berry's phase for a spin-1/2 particle, Phys. Rev. Lett. **102**, 030404 (2009).
  - [15] M. V. Berry, Quantal phase factors accompanying adiabatic changes, Proc. R. Soc. Lond. A **392**, 45 (1984).
  - [16] Y. Aharonov, and J. Anandan, Phase change during a cyclic quantum evolution, Phys. Rev. Lett. **58**, 1593 (1987).
  - [17] F. Wilczek, and A. Zee, Appearance of gauge structure in simple dynamical systems, Phys. Rev. Lett. **52**, 2111 (1984).
  - [18] J. A. Jones, V. Vedral, A. Ekert, and G. Castagnoli, Geometric quantum computation using nuclear magnetic resonance, Nature **403**, 869 (2000).
  - [19] L. M. Duan, J. I. Cirac and P. Zoller, Geometric manipulation of trapped ions for quantum computation, Science **292**, 1695 (2001).

- [20] L.-A. Wu, P. Zanardi, and D. A. Lidar, Holonomic Quantum Computation in Decoherence-Free Subspaces, *Phys. Rev. Lett.* **95**, 130501 (2005).
- [21] J. Anandan, Non-adiabatic non-abelian geometric phase, *Phys. Lett. A* **133**, 171 (1988).
- [22] B.-J. Liu, Z.-H. Huang, Z.-Y. Xue, and X.-D. Zhang, Superadiabatic holonomic quantum computation in cavity QED, *Phys. Rev. A* **95**, 062308 (2017).
- [23] J. Zhang, T. H. Kyaw, D. M. Tong, E. Sjöqvist, and L. C. Kwek, Fast non-Abelian geometric gates via transitionless quantum driving, *Sci. Rep.* **5**, 18414 (2015).
- [24] X.-K. Song, H. Zhang, Q. Ai, J. Qiu, and F.-G. Deng, Shortcuts to adiabatic holonomic quantum computation in decoherence-free subspace with transitionless quantum driving algorithm, *New J. Phys.* **18**, 023001 (2016).
- [25] E. Sjöqvist, D. M. Tong, L. M. Andersson, B. Hessmo, M. Johansson, and K. Singh, Non-adiabatic holonomic quantum computation, *New J. Phys.* **14**, 103035 (2012).
- [26] G. F. Xu, J. Zhang, D. M. Tong, E. Sjöqvist, and L. C. Kwek, Nonadiabatic Holonomic Quantum Computation in Decoherence-free Subspaces, *Phys. Rev. Lett.* **109**, 170501 (2012).
- [27] Z.-Y. Xue, F.-L. Gu, Z.-P. Hong, Z.-H. Yang, D.-W. Zhang, Y. Hu, and J. Q. You, Nonadiabatic holonomic quantum computation with dressed-state qubits, *Phys. Rev. Appl.* **7**, 054022 (2017).
- [28] Abdumalikov, A. A. *et al.* Experimental realization of non-Abelian non-adiabatic geometric gates, *Nature* **496**, 482-485 (2013).
- [29] G. Feng, G. Xu and G. Long. Experimental Realization of Nonadiabatic Holonomic Quantum Computation, *Phys. Rev. Lett.* **110**, 190501 (2013).
- [30] Arroyo-Camejo, S. *et al.* Room temperature high-fidelity holonomic single-qubit gate on a solid-state spin, *Nat. Commun.* **5**, 4870 (2014).
- [31] Li, H., Yang, L. and G. Long. Experimental realization of single-shot nonadiabatic holonomic gates in nuclear spins, *Sci. China-Phys. Mech. Astron.* **60**, 080311 (2017).
- [32] Y. Sekiguchi, N. Niikura, R. Kuroiwa, H. Kano, and H. Kosaka, Optical holonomic single quantum gates with geometric spin under a zero field, *Nat. Photonics* **11**, 309 (2017).
- [33] B. B. Zhou, P. C. Jerger, V. O. Shkolnikov, F. J. Heremans, G. Burkard, and D. D. Awschalom, Holonomic Quantum Control by Coherent Optical Excitation in Diamond, *Phys. Rev. Lett.* **119**, 140503 (2017).
- [34] D. J. Egger, M. Ganzhorn, G. Salis, A. Fuhrer, P. Mueller, P. K. Barkoutsos, N. Moll, I. Tavernelli, and S. Filipp, Entanglement generation in superconducting qubits using holonomic operations, *Phys. Rev. Appl.* **11**, 014017 (2019).
- [35] Y. Xu, W. Cai, Y. Ma, X. Mu, L. Hu, T. Chen, H. Wang, Y. P. Song, Z.-Y. Xue, Z.-Q. Yin, and L. Sun, Single-Loop Realization of Arbitrary Nonadiabatic Holonomic Single Qubit Quantum Gates in a Superconducting Circuit, *Phys. Rev. Lett.* **121**, 110501 (2018).
- [36] Z. Zhu, T. Chen, X. Yang, J. Bian, Z.-Y. Xue, and X. Peng, Single-Loop and Composite-Loop Realization of Nonadiabatic Holonomic Quantum Gates in a Decoherence-Free Subspace, *Phys. Rev. Appl.* **12**, 024024 (2019).
- [37] Z. Han, Y. Dong, B. Liu, X. Yang, S. Song, L. Qiu, D. Li, J. Chu, W. Zheng, J. Xu, T. Huang, Z. Wang, X. Yu, X. Tan, D. Lan, M.-H. Yung, Y. Yu
- [38] M. Johansson, E. Sjöqvist, L. M. Andersson, M. Ericsson, B. Hessmo, K. Singh, and D. M. Tong, Robustness of non-adiabatic holonomic gates, *Phys. Rev. A* **86**, 062322 (2012).
- [39] S. B. Zheng, C. P. Yang, and F. Nori, Comparison of the sensitivity to systematic errors between nonadiabatic non-Abelian geometric gates and their dynamical counterparts, *Phys. Rev. A* **87**, 032326 (2016).
- [40] J. Jing, C.-H. Lam, and L.-A. Wu, Non-Abelian holonomic transformation in the presence of classical noise, *Phys. Rev. A* **95**, 012334 (2017).
- [41] B. J. Liu, X. K. Song, Z. Y. Xue, X. Wang, and M. H. Yung, Plug-and-Play Approach to Nonadiabatic Geometric Quantum Gates, *Phys. Rev. Lett.* **123**, 100501 (2019).
- [42] T. Yan, B.-J. Liu, K. Xu, C. Song, S. Liu, Z. Zhang, H. Deng, Z. Yan, H. Rong, M.-H. Yung, Y. Chen, and D. Yu, Experimental realization of non-adiabatic shortcut to non-Abelian geometric gates, *Phys. Rev. Lett.* **122**, 080501 (2019).
- [43] S. Li, T. Chen, and Z.-Y. Xue, Fast holonomic quantum computation on superconducting circuits with optimal control, *Adv. Quantum Technol.* **3**, 2000001 (2020).
- [44] Y.-H. Kang, Z.-C. Shi, B.-H. Huang, J. Song, and Y. Xia, Flexible scheme for the implementation of nonadiabatic geometric quantum computation, *Phys. Rev. A* **101**, 032322 (2020).
- [45] H. R. Lewis, and W. B. Riesenfeld, An Exact Quantum Theory of the Time-Dependent Harmonic Oscillator and of a Charged Particle in a Time-Dependent Electromagnetic Field, *J. Math. Phys.* **10**, 1458 (1969).
- [46] G. Lindblad, On the generators of quantum dynamical semigroups, *Commun. Math. Phys.* **48**, 119130 (1976).
- [47] R. Barends, J. Kelly, A. Megrant, A. Veitia, D. Sank, E. Jeffrey, T. C. White, J. Mutus, A. G. Fowler, B. Camp- bell *et al.*, *Nature (London)* **508**, 500 (2014).
- [48] Z. Chen, J. Kelly, C. Quintana, R. Barends, B. Campbell, Y. Chen, B. Chiaro, A. Dunsworth, A. G. Fowler, E. Lucero *et al.*, *Phys. Rev. Lett.* **116**, 020501 (2016).